

## High resolution NMR study of T1 magnetic relaxation dispersion. IV. Proton relaxation in amino acids and Met-enkephalin pentapeptide

Andrey N. Pravdivtsev, Alexandra V. Yurkovskaya, Hans-Martin Vieth, and Konstantin L. Ivanov

Citation: *The Journal of Chemical Physics* **141**, 155101 (2014); doi: 10.1063/1.4897336

View online: <http://dx.doi.org/10.1063/1.4897336>

View Table of Contents: <http://scitation.aip.org/content/aip/journal/jcp/141/15?ver=pdfcov>

Published by the [AIP Publishing](#)

---

### Articles you may be interested in

[Pf1 bacteriophage hydration by magic angle spinning solid-state NMR](#)

*J. Chem. Phys.* **141**, 22D533 (2014); 10.1063/1.4903230

[Nuclear magnetic relaxation induced by exchange-mediated orientational randomization: Longitudinal relaxation dispersion for spin  \$I = 1\$](#)

*J. Chem. Phys.* **137**, 054503 (2012); 10.1063/1.4739297

[An integrated approach to NMR spin relaxation in flexible biomolecules: Application to  \$\beta\$  - D -glucopyranosyl- \( 1  \$\rightarrow\$  6 \) -  \$\alpha\$  - D -mannopyranosyl-OMe](#)

*J. Chem. Phys.* **131**, 234501 (2009); 10.1063/1.3268766

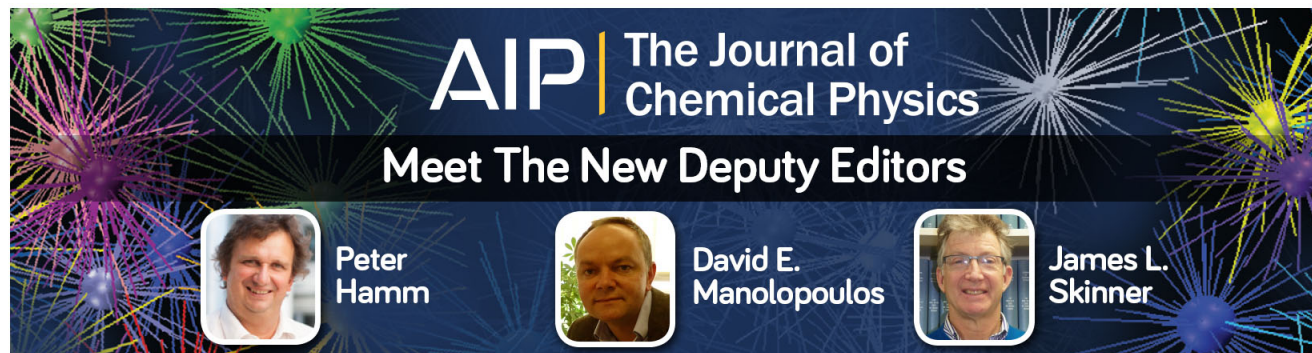
[The magnetic field and temperature dependences of proton spin-lattice relaxation in proteins](#)

*J. Chem. Phys.* **126**, 175105 (2007); 10.1063/1.2727464

[Magnetic relaxation measurement in immunoassay using high-transition-temperature superconducting quantum interference device system](#)




*J. Appl. Phys.* **99**, 124701 (2006); 10.1063/1.2203390

---



**AIP** | The Journal of  
Chemical Physics

### Meet The New Deputy Editors

	<b>Peter Hamm</b>		<b>David E. Manolopoulos</b>		<b>James L. Skinner</b>
---	-------------------	---	------------------------------	---	-------------------------

# High resolution NMR study of $T_1$ magnetic relaxation dispersion.

## IV. Proton relaxation in amino acids and Met-enkephalin pentapeptide

Andrey N. Pravdivtsev,<sup>1,2</sup> Alexandra V. Yurkovskaya,<sup>1,2</sup> Hans-Martin Vieth,<sup>3</sup>  
 and Konstantin L. Ivanov<sup>1,2,a)</sup>

<sup>1</sup>International Tomography Center, Institutskaya 3a, Novosibirsk 630090, Russia

<sup>2</sup>Department of Physics, Novosibirsk State University, Pirogova 2, Novosibirsk 630090, Russia

<sup>3</sup>Institut für Experimentalphysik, Freie Universität Berlin Arnimallee 14, 14195 Berlin, Germany

(Received 12 August 2014; accepted 8 September 2014; published online 16 October 2014)

Nuclear Magnetic Relaxation Dispersion (NMRD) of protons was studied in the pentapeptide Met-enkephalin and the amino acids, which constitute it. Experiments were run by using high-resolution Nuclear Magnetic Resonance (NMR) in combination with fast field-cycling, thus enabling measuring NMRD curves for all individual protons. As in earlier works, Papers I–III, pronounced effects of intramolecular scalar spin-spin interactions, J-couplings, on spin relaxation were found. Notably, at low fields J-couplings tend to equalize the apparent relaxation rates within networks of coupled protons. In Met-enkephalin, in contrast to the free amino acids, there is a sharp increase in the proton  $T_1$ -relaxation times at high fields due to the changes in the regime of molecular motion. The experimental data are in good agreement with theory. From modelling the relaxation experiments we were able to determine motional correlation times of different residues in Met-enkephalin with atomic resolution. This allows us to draw conclusions about preferential conformation of the pentapeptide in solution, which is also in agreement with data from two-dimensional NMR experiments (rotating frame Overhauser effect spectroscopy). Altogether, our study demonstrates that high-resolution NMR studies of magnetic field-dependent relaxation allow one to probe molecular mobility in biomolecules with atomic resolution. © 2014 AIP Publishing LLC. [<http://dx.doi.org/10.1063/1.4897336>]

### I. INTRODUCTION

Field-cycling Nuclear Magnetic Resonance (NMR) relaxometry is a widely used tool to study molecular mobility, which is applicable to a wide range of systems such as molecules in liquid solutions, polymers, molecular crystals, liquid crystals, and biomolecules.<sup>1–11</sup> In such experiments spin relaxation times are measured as a function of the external magnetic field; theoretical modeling of such field dependences, also termed Nuclear Magnetic Relaxation Dispersion (NMRD) curves, enables extracting motional parameters, i.e., motional correlation times,  $\tau_c$ . In general, the rate,  $R_{\mu\nu}$ , of the relaxation transition for a pair of quantum spin states,  $|\mu\rangle$  and  $|\nu\rangle$ , can depend on the external magnetic field for three reasons. First, the spectral density of fluctuations,  $J(\omega_{\mu\nu})$ , can change upon variation of the field and thus of the energy difference,  $\omega_{\mu\nu}$ , for the corresponding pair of levels. In this case, the changes in the relaxation rates are attributed to the change of the motional regime:  $J(\omega_{\mu\nu})$  changes considerably upon going from the limit of fast motion,  $\omega_{\mu\nu}\tau_c \ll 1$ , to the limit of slow motion  $\omega_{\mu\nu}\tau_c \geq 1$ . Second, the fluctuating part of the Hamiltonian,  $\hat{H}_f(t)$ , can be field dependent; a typical example of such situation is given by relaxation caused by fluctuations of the Chemical Shift Anisotropy (CSA). Third, the rate  $R_{\mu\nu}$  can change with the field because the eigen-states,

$|\mu\rangle$  and  $|\nu\rangle$ , change upon field variation. The reason for this is variation of the coupling regime in a network of interacting spins at different fields. This possibility was studied in detail in Papers I–III<sup>12–14</sup> for small molecules, which have several coupled spins. We have shown that at low fields where the spins are “strongly coupled” they tend to relax with a common  $T_1$ -relaxation time despite a large difference in their high-field relaxation times. By “strong coupling” we hereafter imply that for spins  $i$  and  $j$  the difference,  $\delta v_{ij}$ , in their Zeeman interactions with the field is smaller than their scalar spin-spin interaction,  $J_{ij}$ ; otherwise, the spins are coupled only weakly. In addition to the relaxation with a common  $T_1$ , spin-spin interactions result in nuclear spin Level Anti-Crossings (LACs), which manifest themselves<sup>12–14</sup> as sharp features in NMRD curves. Notably, these features have been observed for small molecules, which tumble fast, so that in the whole accessible field range the extreme narrowing condition,  $\omega_{\mu\nu}\tau_c \ll 1$ , was fulfilled. In addition, protons were studied, for which the CSA effects are negligible; thus, that the observed features in NMRD curves were clearly attributed to the effect of spin-spin interactions.

Hence, the presence of spin-spin couplings is an important factor for the relaxation behavior at low-field, which has to be taken into account for analyzing experimental data. So far, experimental studies of “strong coupling” effects on spin relaxation were limited because assessment of this factor requires high-resolution NMR detection in order to measure relaxation times of all individual protons, not only of the total

<sup>a)</sup> Author to whom correspondence should be addressed. Electronic mail: [ivanov@tomo.nsc.ru](mailto:ivanov@tomo.nsc.ru)

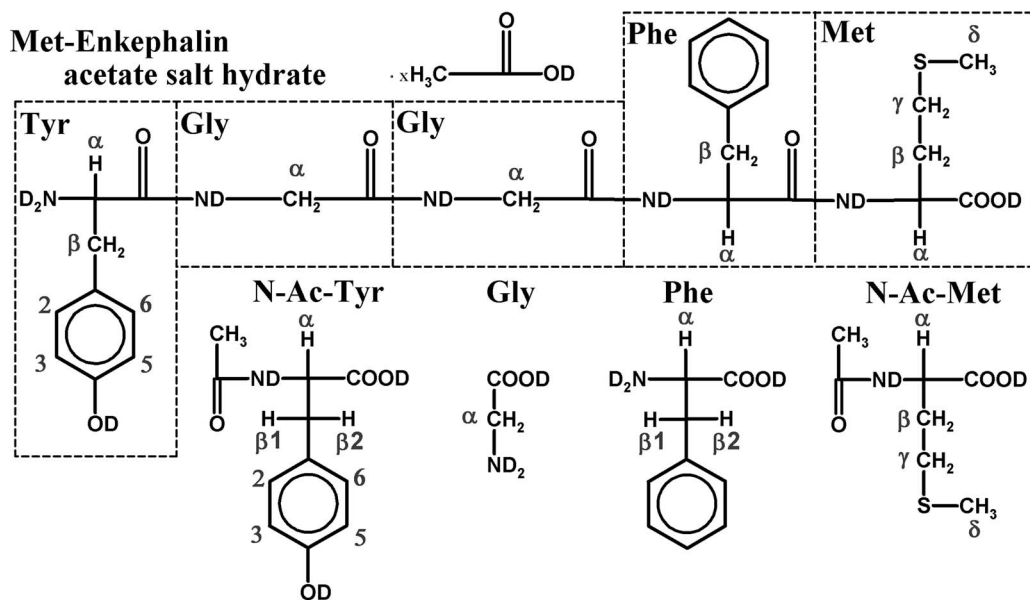


CHART 1. Structure of Met-Enk and the amino acids under study in D<sub>2</sub>O; the five residues of Met-Enk are indicated; assignment of proton positions is also given.

spin magnetization of solvent or solute molecules. This requirement is relatively difficult to fulfill: so far there were only a few investigations dealing with NMR relaxometry with high spectral resolution.<sup>13–20</sup> At the same time, high-resolution studies can open new avenues in NMR relaxometry as they provide site-specific data and thus give a way to probe mobility of individual atoms (or groups of atoms) in a molecule. Field-dependent studies also allow one to assess molecular motions, which cannot be probed by high-field relaxation studies only. Despite a few promising examples<sup>8,18,20,21</sup> of such studies, this attractive possibility has not been fully exploited so far.

Here we report a site-specific NMR relaxometry study of the pentapeptide Met-enkephalin (Met-Enk) and the amino acids, which constitute it: tyrosine (Tyr), two glycines (Gly), phenylalanine (Phe), and methionine (Met). Met-Enk is an endogenous opioid found in the central nervous system and the gastrointestinal tract, which activates opioid receptors in the mammalian pain response pathway.<sup>22</sup> Our study is aimed at probing the mobility of different amino acid residues in Met-Enk and, moreover, of different atoms in each residue. To achieve this goal it is necessary to distinguish features in the NMRD curves, which result from variation of noise spectral densities,  $J(\omega_{\mu\nu})$ , and those conditioned by spin-spin interactions. To this end we also study the free amino acids N-acetyl tyrosine (N-Ac-Tyr), Gly, Phe, and N-acetyl methionine (N-Ac-Met), which have the same spin coupling networks but tumble so fast that for them  $J(\omega_{\mu\nu}) \approx J(0) = \text{const}$  in the whole experimentally accessible magnetic field range. Experiments are done by using a home-built field-cycling device in combination with a high-resolution NMR spectrometer; the data are supported by theoretical modeling, which follows closely the approach we used earlier.<sup>12–14</sup> We show that in Met-Enk the features in the NMRD curves are due to both factors, strong coupling and variation of the motional regime, which are differentiated by taking the data for the amino acids for comparison and by using appropriate theoretical mod-

eling; in addition, site-specific information about molecular mobility is extracted. From the NMRD data, we also draw conclusions about the conformation of Met-Enk in solution and compare the results with those obtained by the ROESY (rotating frame Overhauser effect spectroscopy) technique.<sup>23</sup>

## II. MATERIALS AND METHODS

### A. Compounds studied and sample preparation

Chemical structures of the compounds used are shown in Chart 1; numbering of the individual protons in all compounds studied is also given.

N-Ac-Met, Gly, Phe, N-Ac-Tyr, NaOD, DCl, and glass distilled deuterated water (D<sub>2</sub>O) were received from Sigma-Aldrich. Met-Enk was received from Bachem. The 700  $\mu\text{l}$  solution containing 50 mM of one of amino acids or Met-Enk was prepared by dissolution of the compounds in D<sub>2</sub>O without additional purification; pH was adjusted to 10. All samples were purged with pure nitrogen gas and sealed in a standard 5 mm Pyrex NMR tube. In order to avoid vortex formation and sample shaking during the transfer, a Teflon plug was inserted into the NMR tube on top of the liquid.

The <sup>1</sup>H NMR spectrum of Met-Enk is shown in Figure 1; the assignment of all NMR lines is also given. To make the assignment we used the TOCSY technique.<sup>24</sup> The NMR spectra of the free amino acids (not shown here) are similar to those of the corresponding residues in the peptide. From the spectra we determined NMR parameters such as proton chemical shifts and spin-spin interaction constants; their values are given in the supplementary material (SM)<sup>25</sup> for the free amino acids and the amino acid residues in Met-Enk.

### B. Field-cycling NMR relaxometry

To switch the external magnetic field in a fast and controllable way we used a field-cycling device, which moves

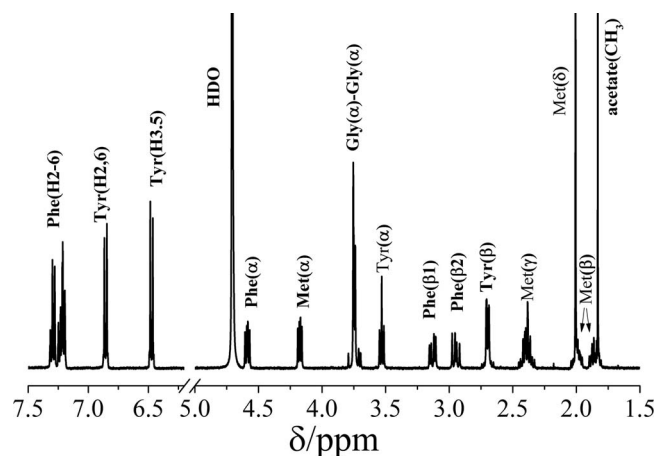


FIG. 1. A 700 MHz proton NMR spectrum of Met-Enk in aqueous solution of pH 10; NMR lines are assigned in the figure.

the whole NMR probehead with the sample in the inhomogeneous fringe field generated by the NMR cryo-magnet and a set of auxiliary electromagnets. The NMR probehead is moved by a digitally controlled step motor, which precisely positions the sample at different magnetic fields. A detailed description of this setup is given in Refs. 26–28; here we only summarize its technical parameters, which are essential in the context of this work. The setup enables high-resolution NMR detection under permanent slow sample rotation (0–150 Hz) at the high field,  $B_0$ , of the NMR spectrometer equal to 7 T; the NMR spectral resolution is about 0.3 Hz. The magnetic field can be set in the range from 0.1 mT to 7 T; in the low-field part of this region, namely, for fields below 0.1 T, the field is controlled with an accuracy of about 0.1 mT. The minimal achievable time of field switching from the highest to the lowest position (and *vice versa*) is 0.27 s; the time profile of field variation,  $B(t)$ , is precisely known. Such a device has been first constructed at the Free University of Berlin (Germany) and is now available at the International Tomography Center (Novosibirsk, Russia).

The NMRD experiments were performed according to the following experimental protocol, which comprises 5 consecutive stages, see Figure 2. In stage 1 the spin system is relaxed to thermal equilibrium at the NMR spectrometer field,  $B_0$ ; the duration of this stage,  $\tau_R$ , is always taken relatively long (from 3 to 5 times the longest  $T_1$ -relaxation time of the protons in the molecule studied) so that all spins acquire their equilibrium magnetization at this field. At the end of stage 1, a  $180^\circ$  RF-pulse is applied and magnetization of all spins is inverted. After that, in stage 2, having a duration of  $\tau_1$  the field is switched from  $B_0$  to the field  $B$ . In our experiments the spin relaxation kinetics is studied at different  $B$  fields. To this end, in stage 3 the spin system is allowed to relax to a new equilibrium at  $B$  during the variable time interval  $\tau$ . Then in stage 4 the field is switched back to the detection position  $B_0$  during time  $\tau_1$ . Finally, in stage 5 a  $90^\circ$  RF-pulse is applied and the free induction decay is measured; its Fourier transformation gives the high-resolution NMR spectrum, in which signals,  $M_i$ , of all individual spins are measured. To assess spin relaxation effects the experiment is repeated 20 times with differ-

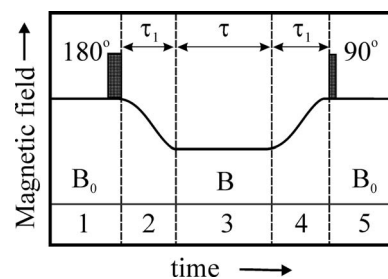


FIG. 2. Experimental protocol used for relaxation measurements. Stage 1 – Preparation; spins relax to thermal equilibrium at the  $B_0$  field, after that, a  $180^\circ$  RF-pulse inverts spin magnetization. Stage 2 – Lowering the field to the field  $B$ . Stage 3 – Letting the spins relax at the field  $B$  during time  $\tau$ . Stage 4 – Going back to the observation field  $B_0$ . Stage 5 – Acquiring the NMR spectrum. See text for detailed explanation.

ent relaxation periods,  $\tau$ , for the same  $B$  value. The functions  $M_i(\tau)$  give the relaxation traces, which are approximated by mono-exponentials to extract the  $T_1$ -relaxation of all spins,  $T_{1i}$ . To obtain field-dependent relaxation data the same experiment is done at different  $B$  field strengths; as a result, the field dependences,  $T_{1i}(B)$ , are obtained for all coupled spins. Typical  $M_i(\tau)$  traces are shown in SM. The time  $\tau_1$  for each  $B$  was taken as short as possible to minimize unwanted relaxation during field switching.

### C. Theoretical model

The calculation method follows closely the one used earlier by us;<sup>12–14</sup> to describe spin relaxation we made use of the Redfield theory.<sup>29</sup> As usual, we split the spin Hamiltonian of the molecule under study into a time-independent part,  $\hat{H}_0$ , which defined the eigen-states of the system, and a fluctuating part,  $\hat{H}_1(t)$ , which causes spin relaxation. The Hamiltonian  $\hat{H}_0$  describes a system of  $N$  scalar coupled protons,

$$\hat{H}_0 = 2\pi \left( - \sum_{i=1}^N \nu_i \hat{I}_{iz} + \sum_{i<j}^N J_{ij} (\hat{\mathbf{I}}_i \cdot \hat{\mathbf{I}}_j) \right). \quad (1)$$

Here  $\nu_i$  is the Zeeman interaction of the  $i$ th spin with the field, which is determined by its chemical shift,  $\delta_i$ :  $\nu_i = \gamma_p B(1 + \delta_i)/2\pi$  (here the proton gyromagnetic ratio,  $\gamma_p$ , is introduced);  $J_{ij}$  is the scalar spin-spin interaction constant for the corresponding pair of spins. The Hamiltonian  $\hat{H}_1(t)$  results in spin relaxation; the rates of relaxation transitions for a pair of levels,  $|\mu\rangle$  and  $|\nu\rangle \neq |\mu\rangle$ , can be defined as follows:

$$R_{\mu\nu} = \int_{-\infty}^{+\infty} \{ \langle \mu | \hat{H}_1(t) | \nu \rangle \langle \nu | \hat{H}_1(t+\tau) | \mu \rangle \}_{Av} \exp(-i\omega_{\mu\nu}\tau) d\tau. \quad (2)$$

Here  $\{ \dots \}_{Av}$  stands for ensemble averaging, while  $\omega_{\mu\nu} = (\omega_\mu - \omega_\nu)$  is given by the difference in the corresponding eigen-values of  $\hat{H}_0$ , which are  $\omega_\mu$  and  $\omega_\nu$ . To calculate the relaxation rates we assumed that spin relaxation is caused by fluctuating local fields,  $\mathbf{B}_i$ , experienced by each spin; as a result, in the absence of coupling (or in the limit of weak coupling) the spins relax with their “intrinsic”  $T_1$ - and  $T_2$ -



relaxation times, which are equal in the extreme narrowing limit and are defined as  $T_{1i} = T_{2i} = \mathcal{T}_i$ . In this situation, the fluctuating part is defined as

$$\hat{H}_1(t) = - \sum_{i=1}^N \gamma_p (B_{ix}(t) \hat{I}_{ix} + B_{iy}(t) \hat{I}_{iy} + B_{iz} \hat{I}_{iz}). \quad (3)$$

As a consequence, the rates  $R_{\mu\nu}$  can be expressed via the matrix elements  $\langle \mu | \hat{I}_{i\alpha} | \nu \rangle$  (here  $\alpha = \{x, y, z\}$ ). We assumed that the interaction with the local magnetic fields is isotropic, consequently,  $\{B_{ix}^2\}_{Av} = \{B_{iy}^2\}_{Av} = \{B_{iz}^2\}_{Av}$ . We also assumed that (i) different components of the local fields are uncorrelated so that  $\{B_{i\alpha} B_{i\beta}\}_{Av} = 0$  ( $\alpha \neq \beta$ ) and (ii) local fields for different nuclei are also uncorrelated, i.e.,  $\{B_{i\alpha} B_{j\beta}\}_{Av} = 0$  ( $i \neq j$ ). Taking this into account, the remaining terms are written as follows:

$$\begin{aligned} & \gamma_p^2 \int_{-\infty}^{+\infty} \{B_{i\alpha}(t) B_{i\alpha}(t + \tau)\}_{Av} \exp(-i\omega\tau) d\tau \\ &= (\tau_{ci} \gamma_p^2 \{B_{i\alpha}^2\}_{Av}) \cdot \left( \frac{J_i(\omega)}{\tau_{ci}} \right) \equiv \frac{1}{\mathcal{T}_i} \frac{J_i(\omega)}{J_i(0)}. \end{aligned} \quad (4)$$

Here we replaced the ensemble-averaged value  $(2\tau_{ci} \gamma_p^2 \{B_{i\alpha}^2\}_{Av})$  by  $1/\mathcal{T}_i$ ; for calculating the noise spectral density,  $J_i(\omega)$ , we always assumed that the noise auto-correlation function decays exponentially. Then  $J_i(\omega) = \frac{2\tau_{ci}}{1+(\omega\tau_{ci})^2}$  with  $\tau_{ci}$  being the motional correlation time for the corresponding spin. For small molecules such as free amino acids, in aqueous solution at room temperature it is sufficient to consider the extreme narrowing case where  $J(\omega)/J(0) \approx 1$ . As a result, the relaxation rate  $R_{\mu\nu}$  takes the form:

$$\begin{aligned} R_{\mu\nu} &= \sum_{i=1}^N \sum_{\alpha=x,y,z} \frac{1}{\mathcal{T}_i} |\langle \mu | \hat{I}_{i\alpha} | \nu \rangle|^2 \frac{J_i(\omega)}{J_i(0)}, \quad (\mu \neq \nu), \\ R_{\mu\mu} &= - \sum_{\nu \neq \mu} R_{\mu\nu}. \end{aligned} \quad (5)$$

Taking these rates we calculated numerically the evolution of the vector,  $\mathbf{p}(\tau)$ , composed of the eigen-state populations and then the evolution of magnetizations,  $M_i(\tau)$ , of all spins in the same way as previously.<sup>12-14</sup> Finally, a single relaxation time,  $T_{1i}$ , and its  $B$ -field dependence were determined for each spin. This simple model correctly reproduces features in the field dependence arising from both “strong coupling” and LACs and also from the variation of the motional regime upon going to high fields. As input parameters for these model one needs to know the NMR parameters such as chemical shifts and scalar couplings and “intrinsic” relaxation times,  $T_{1i}$ . For each molecule under study we determined chemical shifts and J-couplings directly from its NMR spectrum; for determining  $T_{1i}$  we measured high-field  $T_1$ -relaxation times in the standard inversion-recovery experiments. For amino acids we assigned the measured relaxation times to  $\mathcal{T}_i$ ; for Met-Enk we assumed that the measured relaxation time is equal to  $\mathcal{T}_i \cdot (J_i(0)/J_i(\gamma_p B_0))$ . To define  $\frac{J_i(0)}{J_i(\gamma_p B_0)} = 1 + (\gamma_p B_0 \tau_{ci})^2$  we

fitted the experimental NMRD curves and extracted the unknown correlation times,  $\tau_{ci}$ .

As has been mentioned, in our model we consider only relaxation of eigen-state populations; this is an approximation, which has its applicability limits. As we have shown before<sup>12,13</sup> for coupled multi-spin systems it becomes necessary to consider the full relaxation super-operator when the products,  $J_{ij} T_{1i} \ll 1$ . In this situation, spin relaxation is faster than the evolution dictated by J-couplings, i.e., the eigenstates are ill defined on the timescale of relaxation and the influence of spin-spin interactions vanishes. In all the cases treated below the J-couplings are sufficiently large and the approximation of relaxation of states is valid.

Now let us present the experimental results for NMRD in amino acids and Met-Enk.

### III. RESULTS AND DISCUSSION

#### A. NMRD of amino acids

Let us first describe the data obtained for the free amino acids; the NMRD curves for all four amino acids under study are shown in Figure 3. As has been pointed out previously, for amino acids the correlation times for molecular tumbling are so short (namely, about 100–200 ps) that in the whole field range up to 7 T we obtain  $\gamma_p B \tau_c \ll 1$  and  $J_i(\omega)/J_i(0) \rightarrow 1$ . The case of free amino acids is thus suitable for testing effects of J-couplings on relaxation at low fields.

Among the four amino acids under study Gly represents the simplest case as it has only two magnetically equivalent protons. Accordingly, the relaxation time of the Gly protons does not depend on the field because all three factors, which lead to features of the NMRD curves (see the Introduction), are missing in this case. This is exactly the experimentally observed behavior, see Figure 3(c): the  $T_1$ -relaxation time of the  $\alpha$ -CH<sub>2</sub> protons of Gly virtually does not depend on the field.

The other amino acids exhibit a more complex relaxation behavior. Let us first consider N-Ac-Met and then Phe and N-Ac-Tyr.

In N-Ac-Met there are the  $\delta$ -CH<sub>3</sub> group and the acetyl group, which are not coupled to any other protons, and also five protons belonging to the  $\alpha$ -CH,  $\beta$ -CH<sub>2</sub>, and  $\gamma$ -CH<sub>2</sub> groups, which form a coupled network of spins. Due to the absence of coupling to other spins, the relaxation time is field independent for the  $\delta$ -CH<sub>3</sub> protons and the CH<sub>3</sub> protons of the acetyl group. The other protons have considerably different relaxation times at high field, whereas at low fields, they all tend to relax with a common relaxation time, see Figure 3(a). This is because the entire five-spin system is strongly coupled; thus, not the individual spins relax but instead their collective spin states. Our theoretical treatment also predicts that the relaxation times do not change monotonously with the field: for the NMRD of the  $\alpha$ -CH proton one sees a sharp feature around 450 mT. This feature originates from an LAC in the coupled five-spin system: previously it has been shown that LACs cause such features in NMRDs. Unfortunately, we were not able to clearly reveal this feature experimentally. At the same time, such features are well-documented for other

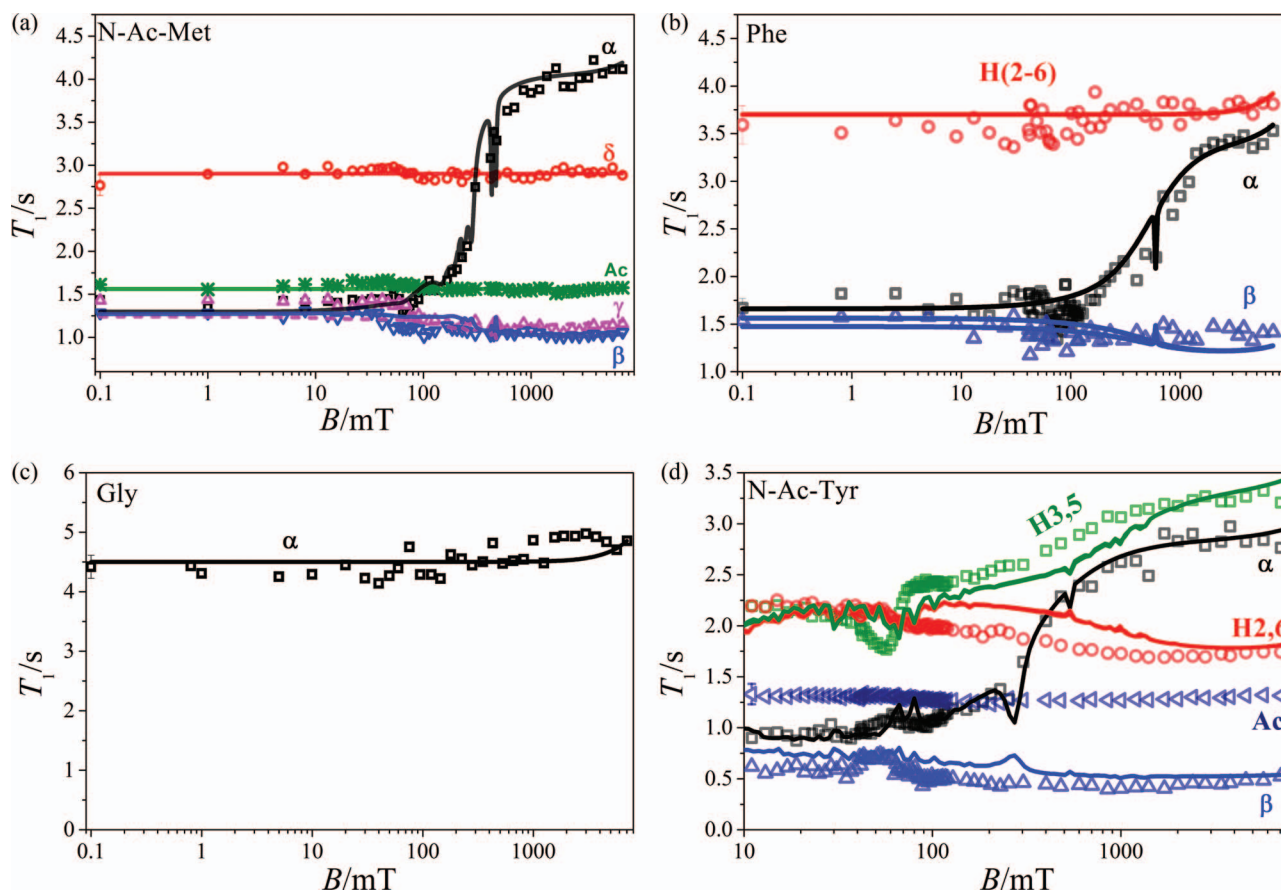


FIG. 3. Proton NMRD curves for four amino acids: (a) N-Ac-Met, (b) Phe, (c) Gly, and (d) N-Ac-Tyr. Lines show the calculation results.

systems;<sup>12–14</sup> studying them in detail is also beyond the scope of this work. Apart from the sharp features, which are relatively difficult to reveal in the present case, the agreement between theory and experiment is very good.

In both N-Ac-Tyr, see Figure 3(d), and Phe, see Figure 3(b), there is a three-spin system formed by the  $\alpha$ -CH proton and two  $\beta$ -CH<sub>2</sub> protons; as follows from our results this system relaxes almost independently of the aromatic protons. The three-spin system also exhibits relaxation with a common  $T_1$  at low fields despite a considerable difference in the high-field relaxation times for the  $\alpha$ -CH proton and the  $\beta$ -CH<sub>2</sub> protons. In addition, there is a sharp feature at intermediate field (250 mT for N-Ac-Tyr and 700 mT for Phe); it is caused by an LAC. It is known that in every system of three non-equivalent spins there is always one of such LACs at a non-zero magnetic field;<sup>12,30</sup> this LAC has a strong effect on the relaxation behavior in the corresponding field range. Different positions of the LAC for N-Ac-Tyr and Phe are due to the different NMR parameters for the two molecules. Specifically, the difference in chemical shifts,  $\delta_\alpha - (\delta_{\beta_1} + \delta_{\beta_2})/2$ , for the  $\alpha$ -CH proton and  $\beta$ -CH<sub>2</sub> protons is three times larger in the case of N-Ac-Tyr, while the scalar coupling between the  $\alpha$ -CH proton and the  $\beta$ -CH<sub>2</sub> protons is about the same in both cases. Therefore, in the case of N-Ac-Tyr the magnetic field where the LAC occurs is approximately three times lower than in Phe. Again, the relaxation behavior is reproduced by the calculation.

As far as the aromatic protons are concerned, in Phe their relaxation time hardly depends on the field due to the

lack of coupling to other spins. In N-Ac-Tyr, at fields below 200 mT the two groups of the aromatic protons, H2,6 and H3,5 protons, start relaxing with a common relaxation time due to strong coupling. In addition, for the H3,5 protons we observed sharp features around 60 mT. The origin of these features is unclear. They might result from rather weak coupling to the  $\beta$ -CH<sub>2</sub> protons; however, in this case our calculation predicts somewhat smaller effects on the relaxation of the aromatic protons. In addition, coupling to the  $\beta$ -CH<sub>2</sub> protons should result in a similar behavior of the H2,6 protons (because at this field the aromatic protons are strongly coupled and relax together), which is not the case in the experiment. Here we leave this issue open. The rest of the relaxation behavior is in good agreement with the simulation.

Having described the relaxation behavior for the free amino acids, let us now consider relaxation in Met-Enk.

## B. NMRD of Met-Enk

NMRD curves for Met-Enk are presented in Figure 4. Relaxation data for the field range were obtained by using the protocol shown in Figure 2. In addition, we measured the relaxation times at two higher fields, 9.4 T and 16.4 T, at 400 MHz and 700 MHz NMR spectrometers by inversion-recovery experiments.

At fields below 1 T, where  $\omega\tau_c \ll 1$ , the NMRD curves for the amino acid residues are essentially the same as those in the corresponding free amino acids: all features in the field

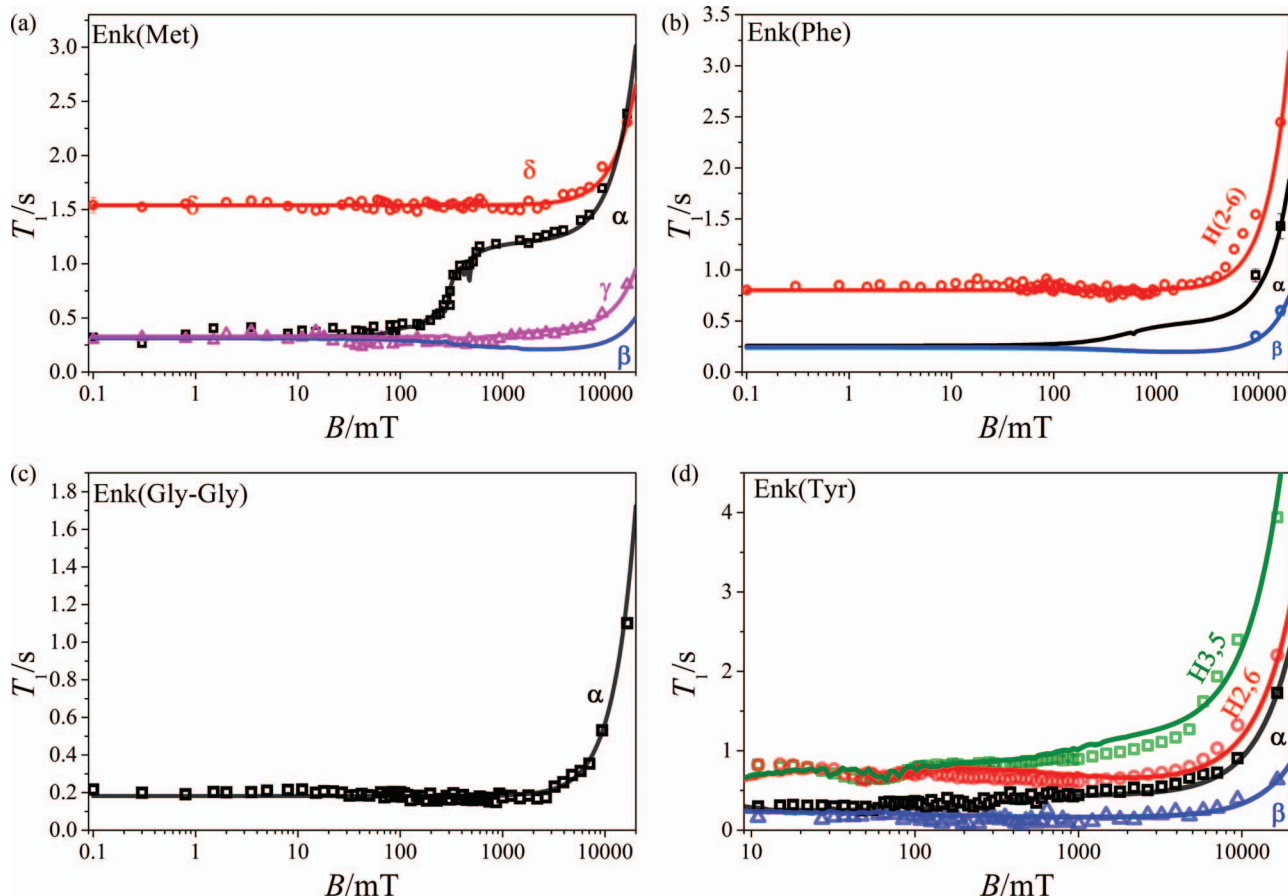


FIG. 4. Proton NMRD curves for Met-Enk shown for different residues: (a) Met ( $\tau_c = 180$  ps for the  $\alpha, \beta, \gamma$ -CH<sub>2</sub> protons and 160 ps for the  $\delta$ -CH<sub>3</sub> protons), (b) Phe ( $\tau_c = 320$  ps), (c) two Gly's ( $\tau_c = 550$  ps), and (d) Tyr ( $\tau_c = 360$  ps). Lines show the calculation results.

dependences of relaxation are originating from strong coupling of spins at low fields and LACs. The only difference is that in the peptide the relaxation times are systematically shorter due to slower molecular motion. At higher fields for all protons of Met-Enk there is a sharp increase of the relaxation times due to the change of the motional regime: from the fast motional limit (extreme narrowing case),  $\omega\tau_c \ll 1$ , at low fields the system goes to the field range where  $\omega\tau_c \sim 1$ . To model such field dependences it is necessary to take into account the variation of  $J(\omega)$  with the field. In turn, from the field dependence of relaxation the motional correlation times can be determined for different residues and even different atoms within the same residue.

We simulated the NMRD curves in the following way. We modeled the data separately for each residue to determine its  $\tau_c$  value. Only for the  $\alpha$ -CH<sub>2</sub> protons of the two Gly residues we considered their total relaxation and determined their average motional correlation time because we were not able to discriminate between their NMR signals. In the case of Met we modelled the NMRD of the  $\delta$ -CH<sub>3</sub> protons completely independent of other nuclei.

As a result of the modelling we determined the following correlation times of motion for the studied residues:  $\tau_c = 180$  ps for the  $\alpha$ -CH and  $\beta, \gamma$ -CH<sub>2</sub> protons of Met and  $\tau_c = 160$  ps for the  $\delta$ -CH<sub>3</sub> protons;  $\tau_c = 320$  ps for Phe;  $\tau_c = 550$  ps for the two Gly's;  $\tau_c = 360$  ps for Tyr. The re-

sults for  $\tau_c$  of different protons are summarized in Table I. One clearly sees that the most mobile residue is Met; furthermore, the  $\delta$ -CH<sub>3</sub> protons of the Met residue are more mobile than the protons, which are closer to the backbone. Tyr and Phe have intermediate mobility in Met-Enk, while the least mobile residues are the Gly's. Previous studies of Met-Enk in bicelles<sup>31</sup> show that the Tyr and Phe residues are surrounding the Gly's, whereas Met is not participating in forming such a structure. The previous experiments<sup>31</sup> were performed in bicelles because for Met-Enk (having rather small size) in the field range 10–20 T we have  $\omega\tau_c \sim 1$ . Consequently, in two-dimensional NMR spectra the NOE (Nuclear Overhauser Effect) cross-peaks, which are necessary to determine the structure, are almost absent not because the atoms are too far apart but rather because the motional conditions in aqueous solution are not favorable for NOE. In bicelles, the correlation times are significantly longer and it becomes possible to determine the NOEs. In addition to the studies in bicelles, we measured the NOE cross-peaks in aqueous solution by using the more

TABLE I. Correlation time of motion,  $\tau_c$ , of individual protons of Met-Enk.

	Met( $\alpha$ -CH and $\beta, \gamma$ -CH <sub>2</sub> )	Met( $\delta$ -CH <sub>3</sub> )	Phe	Gly-Gly	Tyr
$\tau_c$ (ps)	180 ± 16	160 ± 14	320 ± 29	550 + 50	360 ± 32



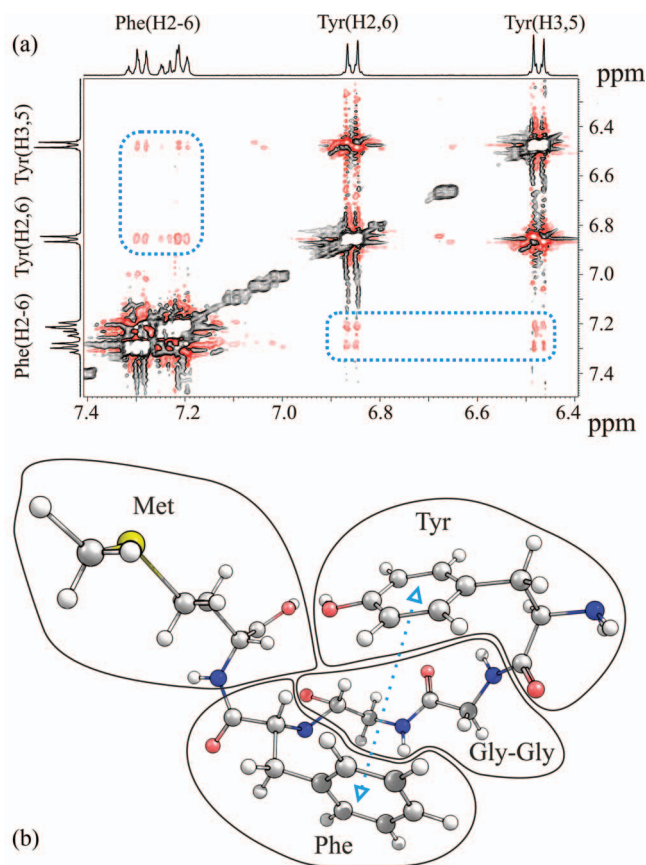


FIG. 5. (a) Aromatic part of the ROESY spectrum of Met-Enk obtained using a 400 MHz NMR spectrometer; cross-peaks between Tyr and Phe rings are highlighted. (b) Structure of Met-Enk obtained by a quantum-chemical calculation performed by ORCA<sup>40</sup> with the hybrid B3LYP functional in the cc-PVDz basis in aqueous solution. Amino acid residues are shown in solid contours; the arrow shows the aromatic groups, whose protons exhibit cross-peaks in the ROESY spectrum, in subplot (a).

sensitive ROESY method.<sup>23,32</sup> This allowed us to obtain the cross-peaks, see Figure 5(a), between the aromatic protons of Tyr and Phe. All other cross-peaks are between atoms belonging to the same amino acid residue and do not add information helpful for determining the secondary structure of Met-Enk. This observation, together with the determined motional correlation times, is in favor of the assumption that in solution the Met-Enk structure is similar to that in bicelles (see Figure 5(b)). In this way, we are able to show that the NMRD data for individual atoms and the resulting motional correlation times provide information on the molecular structure. The conformation (compact conformation with Tyr and Phe in close contact) of Met-Enk revealed by our studies is thought to be bio-active<sup>33</sup> as it is involved in the selection of the receptor.

#### IV. SUMMARY AND CONCLUSIONS

We have studied the NMRD curves for the Met-Enk pentapeptide and the amino acids, which constitute it, in the magnetic field range from 0.1 mT to 16.4 T. The experimental method is based on fast field-cycling and high-resolution NMR detection, which allowed us to obtain the

field-dependent relaxation times for individual protons in the amino acids and in Met-Enk. We have shown that at low fields, 1 T and below, the NMRD curves are determined by scalar spin-spin interactions via the “strong coupling” mechanism. At high field, the relaxation times in the free amino acids become constant (within the experimentally accessible range), whereas in Met-Enk the relaxation times depend on the field because of the variation of the motional regime. From the field dependence within this range motional correlation times were determined for the individual residues. Using these  $\tau_c$  values and the two-dimensional ROESY method we were able to make a conclusion on the structure of Met-Enk in solution. Our site-specific method (meaning that the mobility of individual atoms can be assessed) enables highly detailed characterization of molecular motion.

Our study shows the importance of J-couplings on spin relaxation, which is usually ignored completely. As is clearly shown by the comparison of NMRDs for the free amino acids and the corresponding amino acid residues in Met-Enk, at low fields effects of J-coupling are very pronounced: “strong coupling” forces spins to relax with a common  $T_1$ -relaxation time. This effect cannot be accounted for when uncoupled spins are considered. “Strong coupling” has to be taken into account when analyzing relaxation at low fields: neglecting it prevents interpretation of the data even on the qualitative level. The only case where the spin-spin interactions are irrelevant is given by the situation where spin relaxation proceeds faster than the spin evolution given by J-coupling. In the study of Met-Enk we were able to distinguish clearly the features coming from spin-spin interactions from those caused by molecular motions; the motional correlation times were determined for different residues and, moreover, for different protons within the residues.

It is worth noting that other interactions, for instance, partly non-averaged dipole-dipole interactions can lead to similar effects. Again, in such cases the concept of “strong coupling” at low fields must be used to describe the relaxation behavior at low fields. As a related phenomenon, it is also important to mention coherent polarization transfer in coupled spin system. Although this process is dynamic (in contrast to stochastic spin relaxation) it also relies on strong coupling (because polarization is evenly distributed among strongly coupled spins) and is particularly efficient at LACs.<sup>30,34–39</sup> Thus, both concepts, strong coupling and LACs, are also of importance for other low-field NMR experiments.

#### ACKNOWLEDGMENTS

Financial support by the Russian Science Foundation (Grant No. 14-13-01053) is gratefully acknowledged. H.-M.V. is thankful to the Alexander von Humboldt-Foundation for support.

<sup>1</sup>I. Bertini, Y. K. Gupta, C. Luchinat, G. Parigi, C. Schlörb, and H. Schwalbe, *Angew. Chem., Int. Ed.* **44**, 2223 (2005).

<sup>2</sup>I. Bertini, C. Luchinat, and G. Parigi, *Adv. Inorg. Chem.* **57**, 105 (2005).

<sup>3</sup>D. Canet, *Adv. Inorg. Chem.* **57**, 3 (2005).



- <sup>4</sup>R. B. Clarkson, *Top. Curr. Chem.* **221**, 201 (2002).
- <sup>5</sup>R. Kimmich and E. Ansaldo, *Prog. Nucl. Magn. Reson. Spectrosc.* **44**, 257 (2004).
- <sup>6</sup>G. Kothe and J. Stohrer, in *The Molecular Dynamics of Liquid Crystals*, edited by G. R. Luckhurst and C. A. Veracini (Kluwer, Dordrecht, 1994), p. 195.
- <sup>7</sup>C. Luchinat and G. Parigi, *J. Am. Chem. Soc.* **129**, 1055 (2007).
- <sup>8</sup>M. F. Roberts, Q. Cui, C. J. Turner, D. A. Case, and A. G. Redfield, *Biochemistry* **43**, 3637 (2004).
- <sup>9</sup>L. Calucci and C. Forte, *Prog. Nucl. Magn. Reson. Spectrosc.* **55**, 296 (2009).
- <sup>10</sup>B. V. N. Phani Kumar, V. Satheesh, K. Venu, V. S. S. Sastry, and R. Dabrowski, *Chem. Phys. Lett.* **482**, 239 (2009).
- <sup>11</sup>R. G. Bryant and J.-P. Korb, *Magn. Reson. Imaging* **23**, 167 (2005).
- <sup>12</sup>K. Ivanov, A. Yurkovskaya, and H.-M. Vieth, *J. Chem. Phys.* **129**, 234513 (2008).
- <sup>13</sup>S. E. Korchak, K. L. Ivanov, A. V. Yurkovskaya, and H.-M. Vieth, *J. Chem. Phys.* **133**, 194502 (2010).
- <sup>14</sup>S. E. Korchak, K. L. Ivanov, A. N. Pravdivtsev, A. V. Yurkovskaya, R. Kaptein, and H.-M. Vieth, *J. Chem. Phys.* **137**, 094503 (2012).
- <sup>15</sup>A. Kiryutin, K. Ivanov, A. Yurkovskaya, and H.-M. Vieth, *Solid State Nucl. Mag.* **34**, 142 (2008).
- <sup>16</sup>D. Ivanov and A. Redfield, *Z. Naturforsch., A: Phys. Sci.* **53**, 269 (1998).
- <sup>17</sup>A. G. Redfield, *Magn. Reson. Chem.* **41**, 753 (2003).
- <sup>18</sup>M. F. Roberts and A. G. Redfield, *J. Am. Chem. Soc.* **126**, 13765 (2004).
- <sup>19</sup>A. G. Redfield, *J. Biomol. NMR* **52**, 159 (2012).
- <sup>20</sup>C. Charlier, S. N. Khan, T. Marquardsen, P. Pelupessy, V. Reiss, D. Sakellariou, G. Bodenhausen, F. Engelke, and F. Ferrage, *J. Am. Chem. Soc.* **135**, 18665 (2013).
- <sup>21</sup>M. F. Roberts and A. G. Redfield, *Proc. Nat. Acad. Sci. U.S.A.* **101**, 17066 (2004).
- <sup>22</sup>J. Malicka, C. Czaplewski, M. Groth, W. Wiczak, S. Oldziej, L. Lankiewicz, J. Ciarkowski, and A. Liwo, *Curr. Top. Med. Chem.* **4**, 123 (2004).
- <sup>23</sup>A. G. Palmer III, W. J. Fairbrother, J. Cavanagh, N. J. Skelton, and M. Rance, *Protein NMR Spectroscopy: Principles and Practice*, 2nd ed. (Academic Press, 2005).
- <sup>24</sup>L. Braunschweiler and R. R. Ernst, *J. Magn. Reson.* **53**, 521 (1983).
- <sup>25</sup>See supplementary material at <http://dx.doi.org/10.1063/1.4897336> for NMR parameters of the compounds under study.
- <sup>26</sup>S. Grosse, F. Gubaydullin, H. Scheelken, H.-M. Vieth, and A. V. Yurkovskaya, *Appl. Mag. Reson.* **17**, 211 (1999).
- <sup>27</sup>S. Grosse, A. V. Yurkovskaya, J. Lopez, and H.-M. Vieth, *J. Phys. Chem. A* **105**, 6311 (2001).
- <sup>28</sup>S. E. Korchak, Hyperpolarization in Coupled Multi-Spin Systems. Ph.D. thesis, Freie Universität Berlin, Berlin, 2010.
- <sup>29</sup>A. G. Redfield, in *Advances in Magnetic Resonance*, edited by J. S. Waugh (Academic, New York, 1965), p. 1.
- <sup>30</sup>K. Miesel, K. L. Ivanov, A. V. Yurkovskaya, and H.-M. Vieth, *Chem. Phys. Lett.* **425**, 71 (2006).
- <sup>31</sup>I. Marcotte, F. Separovic, M. Auger, and S. M. Gagné, *Biophys. J.* **86**, 1587 (2004).
- <sup>32</sup>J. Kowalewski, and L. Maler, *Nuclear Spin Relaxation in Liquids: Theory, Experiments, and Applications* (Taylor & Francis Group, Boca Raton, 2006), p. 426.
- <sup>33</sup>R. Schwyzer, *Biochemistry* **25**, 6335 (1986).
- <sup>34</sup>L. Buljubasich, M. B. Franzoni, H. W. Spiess, and K. Münnemann, *J. Magn. Reson.* **219**, 33 (2012).
- <sup>35</sup>L. Buljubasich, I. Prina, M. B. Franzoni, K. Münnemann, H. W. Spiess, and R. H. Acosta, *J. Magn. Reson.* **230**, 155 (2013).
- <sup>36</sup>M. B. Franzoni, L. Buljubasich, H.-W. Spiess, and K. Münnemann, *J. Am. Chem. Soc.* **134**, 10393 (2012).
- <sup>37</sup>A. N. Pravdivtsev, A. V. Yurkovskaya, R. Kaptein, K. Miesel, H.-M. Vieth, and K. L. Ivanov, *Phys. Chem. Chem. Phys.* **15**, 14660 (2013).
- <sup>38</sup>A. N. Pravdivtsev, A. V. Yurkovskaya, H.-M. Vieth, and K. L. Ivanov, *J. Chem. Phys.* **139**, 244201 (2013).
- <sup>39</sup>A. N. Pravdivtsev, A. V. Yurkovskaya, H.-M. Vieth, K. L. Ivanov, and R. Kaptein, *ChemPhysChem* **14**, 3327 (2013).
- <sup>40</sup>F. Neese, *WIREs Comput. Mol. Sci.* **2**, 73–78 (2012).